Synthesis and Direct Topology Visualization of High-Molecular-Weight Star PMMA

L. Xue,[†] U. S. Agarwal,*[,†] M. Zhang,[‡] B. B. P. Staal,[†] A. H. E. Müller,[‡] C. M. E. Bailly,[§] and P. J. Lemstra[†]

Faculty of Chemical Engineering, Eindhoven University of Technology, 5600 MB, Eindhoven, The Netherlands, Makromolekulare Chemie II, Universität Bayreuth, D-95440 Bayreuth, Germany, and Laboratory of Macromolecular Structureal Chemistry, Unité de Physique et de Chimie des Hauts Polymères, Université Catholique de Louvain, roix du Sud, 1, B-1348 Louvain-la-Neuve, Belgium

Received July 23, 2004; Revised Manuscript Received December 15, 2004

ABSTRACT: We report synthesis and direct topology visualization of single molecules of six-arm star poly(methyl methacrylate) (PMMA). We synthesized two hexafunctional initiators, 2,3,6,7,10,11-triphenylene hexa-2-bromo-2-methylpropionate (fused-core initiator) and ethylene glycol bis[3,4,5-tri(2-bromo-2-methylpropionate)] benzoylate (linear-core initiator). Their structures differ in the linking arrangement of the initiating sites. Atom transfer radical polymerizations (ATRP) of methyl methacrylate (MMA) from these initiators using CuCl as the catalyst and 4,4′-di-*n*-nonyl-2,2′-bipyridine as the ligand at 90 °C produced six-arm star PMMAs with very high molecular weight ($\bar{M}_w$ > 2 million) and narrow molecular weight distribution (polydispersity index ≈ 1.3). A high initiation efficiency (>90%) of the initiating sites is inferred from a good match of the $\bar{M}_w$ of the star PMMA with the expected value based on $\bar{M}_w$ of the cleaved arms. SEC-LS analysis confirmed the compact structure of the star PMMA compared to linear PMMA and the absence of star-star coupling. Tapping mode scanning force microscopy of a dip-coated sample on mica enabled resolution of the individual arms linked to the initiating core and allowed clear identification of predominantly six-arm star molecules.

Introduction

High-molecular-weight polymers with controlled architectures are desirable for applications such as rheology modifications,[1−5] as well as control of crystallization characteristics, morphology development, and mechanical performance.[2,6−8] Star polymers are of interest because they have an elementary branching topology, with multiple linear chains linked to a single core. To investigate the effect of the structure of the core, it is desired to synthesize star polymers with core structures differing in linking arrangement of the arms, with uniform arm lengths and number of arms. Strategies toward making well-defined star polymers follow one of the two routes. In the "arm-first" approach, monofunctional linear chains are first synthesized by "living"/controlled polymerization methods and then coupled to multifunctional cross-linking agents to form the star polymers. In the "core-first" approach, plurifunctional initiators are used to grow arms by "living"/controlled polymerization methods. Several researchers have described the use of atom transfer radical polymerization (ATRP) for synthesis of star polymers by this core-first approach.[9−14] In addition to the necessary high initiation efficiency required for the core-first approach,[15] synthesis of high-molecular-weight star polymers demands low extent of chain transfer and termination reactions[12] while maintaining a moderate reaction rate. We recently reported good control during a one-pot ATRP from a model unifunctional initiator, 2-bromo-2-methylpropionate, in a system with high monomer-to-initiating site ratio ($[M]_o/[I]_o$ = 6400), leading to linear poly(methyl methacrylate) (PMMA) of high molecular weight ($\bar{M}_n \approx$ 367 000) and low polydispersity index (PDI ≈ 1.2).[16] In this paper, we first report the synthesis of two hexafunctional initiators: 2,3,6,7,10,11-triphenylene hexa-2-bromo-2-methylpropionate (fused-core initiator, TP6Br) and ethylene glycol bis[3,4,5-tri(2-bromo-2-methylpropionate)] benzoylate (linear-core initiator, EG(Bz3Br)$_2$). We then use the well-optimized ATRP conditions to synthesize high-molecular-weight fused-core and linear-core star PMMAs by growing arms from these two hexafunctional initiators. The control of the ATRP processes is evaluated by following the growth of the molecular weight of the stars. In addition, the growth characteristics of the arms is independently evaluated by size exclusion chromatography (SEC) and matrix assisted laser desorption ionization time-of-flight mass spectrometry (MALDI-TOF-MS) of the linear arms cleaved from the star PMMA at the core. The efficiency of initiation from the hexafunctional cores is characterized by relating the weight-average molecular weight ($\bar{M}_w$) of the cleaved arms with the $\bar{M}_w$ of the stars determined by light scattering (SEC-LS). Tapping mode scanning force microscopy (SFM) is used to directly examine the topology of the star PMMA.

Experimental Section

^{1}H NMR Measurements. ^{1}H NMR spectra were recorded on a Varian Mercury Vx 400 spectrometer at 400 MHz using $CDCl_3$ as solvent.

Size Exclusion Chromatography (SEC) and Coupling with Light Scattering (SEC-LS). Average molecular weights and radii of gyration were measured by SEC and SEC-LS coupling using a Waters GPC equipped with a Waters 510 (SEC) or Waters 6000 A (SEC-LS coupling) pump, Waters 410 differential refractometer (at 40 °C, wavelength = 930 nm), and Waters WISP 712 autoinjector with injection volume of 50 (SEC) or 150 μL (SEC-LS). Columns for SEC measurements were one PLgel (5 μm particle size) 50 mm × 7.5 mm guard

* Author to whom correspondence should be addressed. E-mail: u.s.agarwal@tue.nl.
† Eindhoven University of Technology.
‡ Universität Bayreuth.
§ Université Catholique de Louvain.

10.1021/ma0484936 CCC: $30.25
Published on Web 00/00/0000 PAGE EST: 7.8

column and two PLgel mixed-C (5 μm particle size, for 200 to 2×10^6 g/mol) 300 mm × 7.5 mm columns (40 °C). Columns for SEC-LS coupling were a Waters Filter guard column and four Styragel 300 mm × 7.8 mm columns (HR5, HR4, HR3 and HR2 for 5×10^4−4×10^6, 5×10^3−6×10^5, 5×10^2−3×10^4, and 5×10^2−2×10^4 g/mol, respectively). Data acquisition and processing were performed using the Waters Millennium 32 (v3.2) software. Tetrahydrofuran (THF, Biosolve, stabilized with BHT) was used as eluent at a flow rate of 1.0 mL/min. SEC calibration was done using polystyrene (PS) standards (Polymer Laboratories, 580 to 7.1×10^6 g/mol), and molecular weights were recalculated using the universal calibration principle and Mark−Houwink parameters (PS: $K = 1.14 \times 10^{-4}$ dL/g, $\alpha = 0.716$; PMMA: $K = 0.944 \times 10^{-4}$ dL/g, $\alpha = 0.719$).[17] For SEC-LS coupling, a Dawn DSP-F multi-angle laser light scattering detector (source is a 5 mV linearly polarized He−Ne laser at 632.8 nm) from Wyatt was used and data processed with the Wyatt Astra (v4.72.03) software. Absolute molecular weights were calculated with the help of Zimm plots (refractive index increment $dn/dc = 0.086$ mL/g).[18] An anionically polymerized linear PMMA sample ($\bar{M}_w \approx$ 830 000, Polymer Laboratories) was used as reference.

Matrix Assisted Laser Desorption Ionization Time-of-Flight Mass Spectrometry (MALDI-TOF-MS). The polymer sample solution was prepared in THF at a concentration of 1 mg/mL. The matrix used was *trans*-2-[3-(4-*tert*-butylphenyl)-2-methyl-2-propenylidene] malononitrile. The matrix solution in THF was prepared at a concentration of 40 mg/mL. Silver trifluroacetate (cationic ionization agent, Aldrich, 98%) solution in THF was prepared at a concentration of 1 mg/mL. In a typical MALDI experiment, solutions of the polymer sample, the matrix, and the salt were premixed in the ratio: 5 μL sample: 5 μL matrix:0.5 μL salt. Approximately 0.5 μL of the obtained mixture was hand-spotted on the target plate. All of the spectra were acquired on the Voyager DE-STR (Applied Biosystems) in the linear mode under high vacuum ($<1.37 \times 10^{-6}$ Pa). The frequency of the laser is 20 Hz, and the voltage is 25 000 V. For each spectrum, 1000 laser shots were accumulated.

Scanning Force Microscopy (SFM). SFM images were recorded on a Digital Instruments Dimension 3100 microscopy operated in Tapping Mode (free amplitude of the cantilever ≈ 20 nm, spring constant = 42 N/m, drive amplitude = 277.4 mV, amplitude set point ≈ 0.98). The standard silicon nitride probes (Olympus, OMCL-AC160TS) were driven at 3% offset below their resonance frequencies in the range of 250−350 kHz. Height and phase images were taken at tip velocity of 4 μm/sec. The SFM measurements were performed in the common laboratory conditions. The sample was prepared by dip-coating from a dilute THF solution of the star PMMA onto freshly cleaved mica. To prevent polymer from aggregating during the solvent evaporation, a very dilute solution (4 mg/L, lower than the overlapping concentration by orders of magnitude) was used.

Materials. 2,3,6,7,10,11-Hexamethoxytriphenylene (TP6OMe) (Aldrich, 99%), boron tribromide solution in dichloromethane (Aldrich, 1.0 M, >99%), triethylamine (Merck, >99%), 2-bromoisobutyryl bromide (Merck, >98%), 3,4,5-trihydroxybenzoic acid (gallic acid, Aldrich, 97%), anhydrous tetrahydrofuran (Aldrich, inhibitor free, 99.5+%), anhydrous ethylene glycol (Aldrich, 99.8%), 4-pyrrolidinopyridine (Aldrich, 98%), dicyclohexylcarbodiimide (DCC) (Merck, >99%), and silica gel 60 (0.040−0.063 mm) (Merck) were used as received. Methyl methacrylate (MMA) (Aldrich, 99%) was passed through a basic activated alumina column, extracted with NaOH (5 wt% aqueous), washed with water, dried, and distilled just before use. CuCl (Aldrich, 99.995%) was refluxed with glacial acetic acid, washed with absolute ethanol, and dried in a vacuum oven at 100 °C for 3 days. Xylene (Biosolve, 99%) was distilled from CaH_2 before use. 4,4′-Di-*n*-nonyl-2,2′-bipyridine (d*n*Nbpy) (Aldrich, 97%) was recrystallized from absolute ethanol and dried in a vacuum oven at 40 °C overnight.[16]

Synthesis of 2,3,6,7,10,11-Triphenylene Hexa-2-bromo-2-methylpropionate (TP6Br). TP6OMe was hydrolyzed into 2,3,6,7,10,11-hexahydroxytriphenylene (TP6OH) according to the literature method;[19] the product was recrystallized from deionized water and dried in a vacuum oven under N_2. TP6OH (0.56 g, 1.7 mmol), anhydrous tetrahydrofuran (30 mL), and triethylamine (2.4 mL, 17 mmol) were charged into a dry 100 mL three-neck round-bottom reaction flask equipped with a stirring bar. 2-Bromoisobutyryl bromide (2.0 mL, 16 mmol) was then added dropwise through a dropping funnel with stirring at 0 °C. The solution was stirred overnight, slowly warmed to room temperature, filtered and extracted three times using saturated aq $NaHCO_3$/diethyl ether = 3, v/v, and washed with deionized water, dried over anhydrous $MgSO_4$, and vacuum-dried at 40 °C before use. ^{1}H NMR: δ 8.31 (s, 6 H, **Ar**), 2.16 (s, 36 H, −**CH$_3$**) ppm.

Synthesis of 3,4,5-Tri(2-bromo-2-methylpropionate)] Benzoic Acid (Bz3Br). 2-Bromoisobutyryl bromide (20 g, 0.087 mol) and anhydrous THF (20 mL) were added into a dry three-neck round-bottom reaction flask equipped with a stirring bar and an ice bath. Triethylamide (5.9 g, 0.059 mol) was added with stirring. After the reaction was stirred for 0.5 h, 3,4,5-trihydroxybenzoic acid (1.0 g, 5.9 mmol) solution in anhydrous THF (20 g) was added dropwise through a dropping funnel. The solution was stirred overnight and slowly warmed to room temperature. The product was filtered and extracted with diethyl ether/water, rotary evaporated, and then vacuum-dried for 48 h. ^{1}H NMR: δ 7.91 (s, 2H, **Ar**), 2.08 (s, 18H, −**CH$_3$**) ppm.

Synthesis of Ethylene Glycol Bis[3,4,5-tri(2-bromo-2-methylpropionate)] Benzoylate (EG(Bz3Br)$_2$). Bz3Br (2.0 g, 3.2 mmol), ethylene glycol (94 mg, 1.5 mmol), and 4-pyrrolidinopyridine (45 mg, 0.30 mmol) were dissolved in dry chloroform (10 g), and DCC (0.64 g, 3.2 mmol) solution in chloroform (10 mL) was added while stirring. After being stirred for 2 h, the solution was filtered and then purified by column chromatography over silica gel (0.040−0.063 mm), using (hexane/diethyl ether = 3:2, v/v) as eluent, and subsequent crystallization from this eluent gave EG(Bz3Br)$_2$. ^{1}H NMR: δ 7.85 (s, 4H, **Ar**), 4.69 (s, 4H, −**CH$_2$CH$_2$**−), 2.06 (s, 36H, −**CH$_3$**) ppm.

Typical ATRP Procedure. For ATRP of fused-core star PMMA with monomer-to-initiating site ratio ($[M]_o/[I]_o$ = 16 333), MMA (98 g, 0.98 mol), d*n*Nbpy (0.36 g, 0.87 mmol) and CuCl (0.046 g, 0.46 mmol) were charged into a reaction flask and purged with dry argon for 1 h. TP6Br (0.01 g, 0.01 mmol) was charged into another flask, diluted with xylene (10 mL), purged with dry argon for 1 h, and transferred dropwise over 3 min to the reaction flask. The reaction flask was then immersed into an oil bath preheated to 90 °C. The reaction mixture was stirred for 265 min. Samples were withdrawn with a syringe at desired times. Each sample was dissolved in THF, and the molecular weight distribution was determined by using SEC without further purification. With increasing viscosity, the stirring bar did not mix the reaction mixture efficiently after 125 min. However, the reaction continued, and the last sample was collected at 265 min with a spatula.

Precipitation Fractionation. When mentioned, the star polymer was purified by fractional precipitation. The fused-core star PMMA ($\bar{M}_w \approx 2.35 \times 10^6$) was dissolved in THF (400 mL) at a concentration of ∼3 wt% and heated to 50 °C. *n*-Heptane (200 mL) was added gradually to the hot-stirred solution. High-molecular-weight fraction (∼12 g) precipitated first upon slow cooling to room temperature.

Cleavage of the Arms of the Star PMMA. The star PMMA (10 mg) was dissolved in THF (10 mL). Methanol (2 mL) and NaOH (1 mg) were added, and the solution was refluxed overnight at 80 °C to trans-esterify the ester groups at the core of the star PMMA. After evaporating to dryness, the cleaved product was analyzed by using SEC, MALDI-TOF-MS, SEC-LS, and ^{1}H NMR.

Results and Discussion

Synthesis of the Hexafunctional Initiators. Scheme 1 outlines the synthesis of the fused-core hexafunctional initiator and its use to prepare the fused-core six-arm star PMMA. The commercially available

Scheme 1. Synthesis of Fused-core Hexafunctional Initiator, 2,3,6,7,10,11-Triphenylene Hexa-2-bromo-2-methylpropionate (TP6Br) and the "Core-First" Atom Transfer Radical Polymerization (ATRP) of the Fused-Core Star PMMA[a]

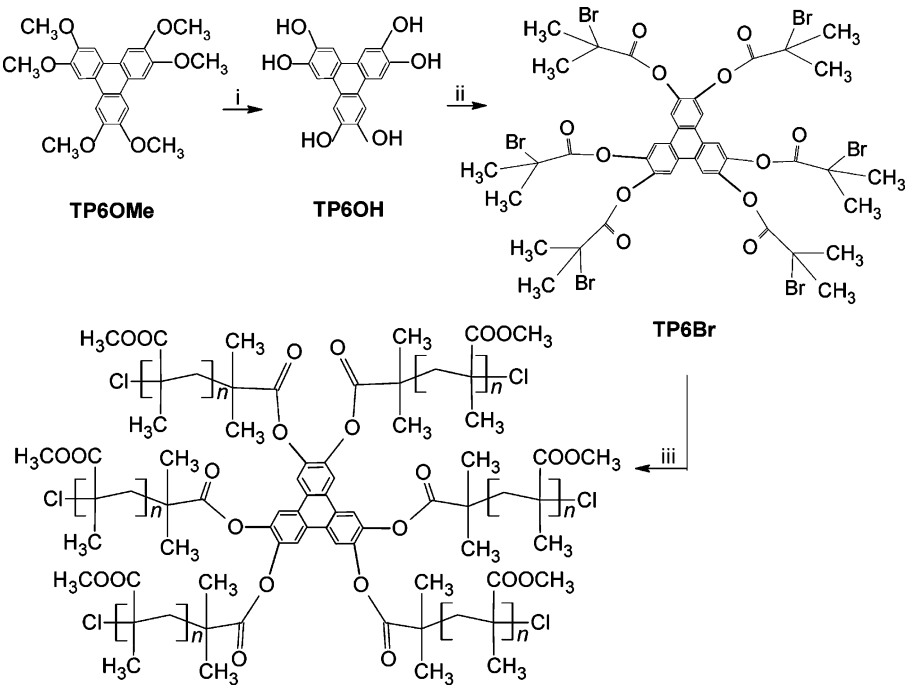

[a] i. 6 BBr_3/H_2O; ii. 6 $Br(CO)C(CH_3)_2Br/N(Et)_3$; iii. MMA, Cu(I)Cl/d*n*Nbpy.

TP6OMe containing six methoxy groups attached to triphenylene were hydrolyzed to give TP6OH containing six hydroxyl functional groups.[19] The ATRP initiating groups with −Br functionality were linked to each of the hydroxyl groups of TP6OH by an esterification reaction to form the hexafunctional fused-core initiator (TP6Br, named to indicate the linking structure between the ATRP initiating sites).

Figure 1 shows the ^1H NMR spectrum of this esterification product: the signal at 8.31 ppm is characteristic of the aromatic protons and the signal at 2.16 ppm of the methyl protons located in the α-position to bromines. There is no signal left at 7.7 or 7.75 ppm corresponding to the aromatic protons in TP6OH or TP6OMe, respectively,[19] indicating quantitative esterification.

Scheme 2 outlines the two-step preparation of the linear-core ATRP initiator, where three initiating groups with −Br functionality were first linked to gallic acid to give Bz3Br. Two of the acid-functionalized Bz3Br molecules were then coupled to ethylene glycol to form the linear core hexafunctional initator, named $EG(Bz3Br)_2$ to indicate its central linear structure linking the two sets of three initiating sites each.

The ^1H NMR spectra of the coupling product $EG(Bz3Br)_2$ and its precursor Bz3Br are shown in Figure 2. The signals at 7.91 and 2.08 ppm are assigned to the aromatic and methyl protons in the precursor Bz3Br. After the coupling reaction with ethylene glycol, the signals shift to 7.85 and 2.06 ppm, respectively, with the appearance of a new signal at 4.69 ppm corresponding to the ethylene protons in the linear-core initiator $EG(Bz3Br)_2$. The disappearance of the signal at 7.91 ppm of the precursor Bz3Br indicates quantitative coupling.

ATRP of Fused-Core Star PMMA. Well-defined fused-core star PMMA were synthesized by ATRP from the fused-core initiator (Scheme 1), using a high monomer-to-initiating site ratio ($[M]_o/[I]_o = 3400$), with CuCl as the catalyst and d*n*Nbpy as the ligand. Figure 3a shows that the SEC-determined $\bar{M}_w$ of star PMMA increases continuously with the time of reaction, while maintaining a low PDI. SEC columns separate polymers according to their hydrodynamic volumes.[20] Since SEC is calibrated with linear polymer standard samples, it underestimates the molecular weight of the star poly-

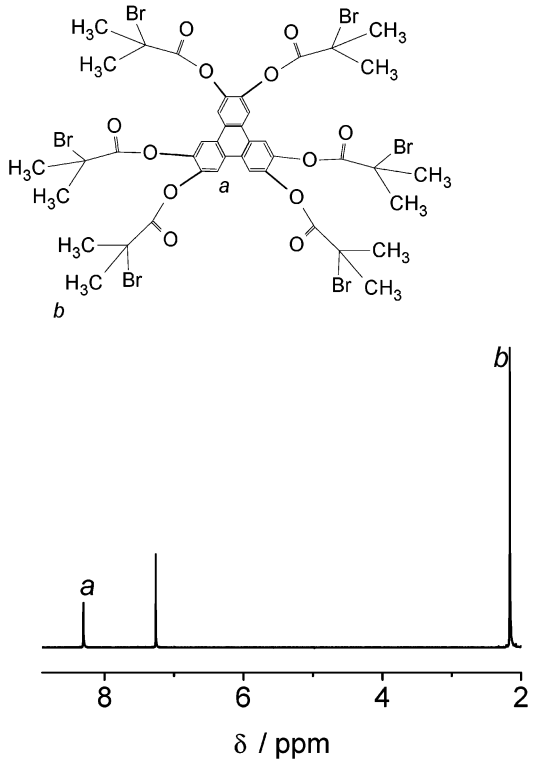

Figure 1. ^1H NMR spectrum of the fused-core initiator 2,3,6,7,10,11-triphenylene hexa-2-bromo-2-methylpropionate (TP6Br) in $CDCl_3$.

Scheme 2. Synthesis of Linear-Core Hexafunctional Initiator Ethylene Glycol Bis[3,4,5-tri(2-bromo-2-methylpropionate)] Benzoylate (EG(Bz3Br)$_2$) and the "Core-First" Atom Transfer Radical Polymerization (ATRP) of the Linear-Core Star PMMA[a]

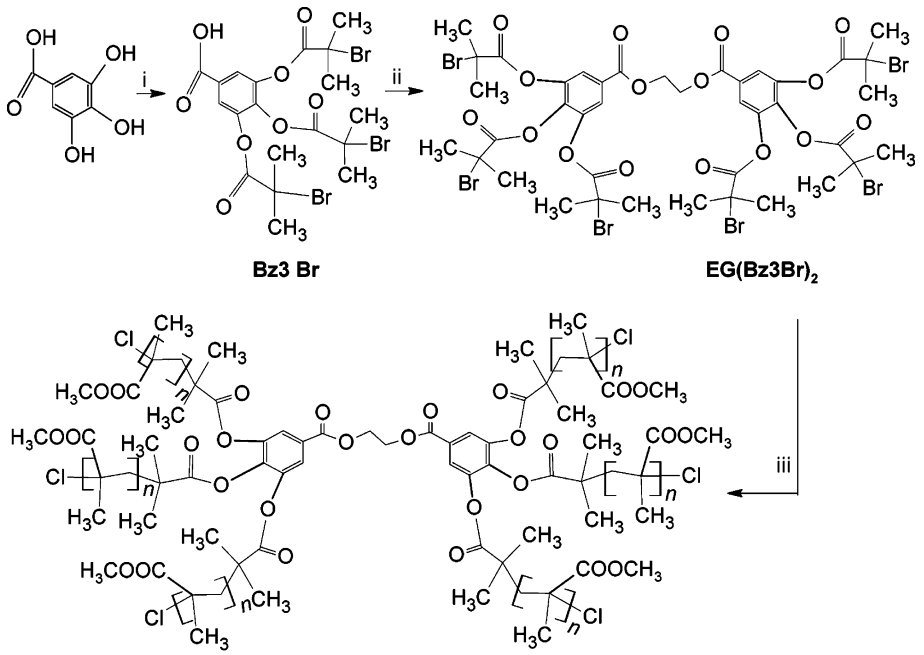

[a] i. 3 BrCOC(CH$_3$)$_2$Br/N(Et)$_3$; ii. 1/2 Ethylene glycol/dicyclohexylcarbodiimide/4-pyrrolidinopyridine; iii. MMA, Cu(I)Cl/d*n*Nbpy.

mers due to their compact volumes compared to the linear chains with the same molecular weight. However, theoretical predictions of macromolecular volumes based on their conformations allow us to estimate the true molecular weight of a star polymer (M_s) of known architecture (f arms) from the apparent molecular weight (M_l) measured in SEC calibrated with linear polymer: [21−23]

$$\frac{M_l}{M_s} = \left(\frac{f^{1/2}}{\sqrt{2}(f-1) - f + 2}\right)^{3/(1+\alpha)} \qquad (1)$$

where $\alpha = 0.719$ for PMMA in THF[17] is the Mark−Houwink constant. This suggests that the molecular weight of a six-arm star polymer (M_s) should be 1.48 times the molecular weight values (M_l) shown in Figure 3a as values measured by SEC calibrated with linear polymers. We therefore also used SEC-LS to determine the absolute $\bar{M}_w$ of the final sample (125 min) of the fused-core star PMMA as 535 000. This is 1.41 times the $\bar{M}_w$ of the same sample as determined by SEC (Figure 3a, $\bar{M}_w \approx 380\,000$) calibrated with linear polymers, and thus in agreement with the theoretical prediction (eq 1)

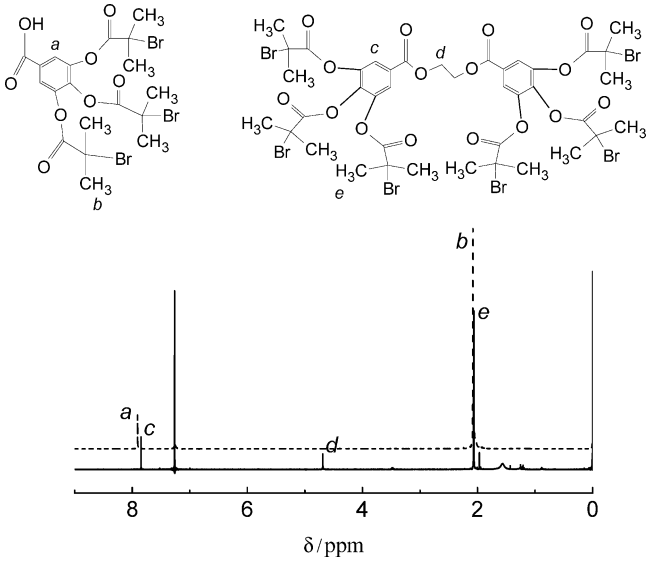

Figure 2. ^{1}H NMR spectra of linear-core initiator ethylene glycol bis[3,4,5-tri(2-bromo-2-methylpropionate)] benzoylate (EG(Bz3Br)$_2$, solid line) and its precursor 3,4,5-tri(2-bromo-2-methylpropionate)] benzoic acid (Bz3Br, dashed line) in $CDCl_3$.

We also evaluated the progress of the ATRP by carrying out cleavage of the arms by transesterification of the ester groups at the core of the star PMMA samples withdrawn during the polymerization at various times. The $\bar{M}_w$ of the cleaved arms was then characterized by SEC and MALDI-TOF-MS. Figure 3b shows that the $\bar{M}_w$ of the cleaved arms also increased during the reaction, while the PDI remained low, again indicating that the ATRP proceeded in a controlled manner. The $\bar{M}_w$ values determined by MALDI-TOF-MS are about 10% higher than the corresponding values determined by SEC. This could be related to the limited accuracy of the universal calibration employed in SEC measurements or to some molecular weight dependence of the ionization efficiency during MALDI-TOF-MS. The arm $\bar{M}_w$ values further permit us to estimate the $\bar{M}_w$ of the star polymers by considering that six arms make up each of the star PMMA. These estimates are also plotted in Figure 3a. When the so-estimated value of the star PMMA (Figure 3a) from the MALDI-TOF-MS data of the arms is extrapolated to higher reaction times, the value at 125 min seems to correspond well with the $\bar{M}_w$ of the star PMMA directly determined by SEC-LS. This indicates a high efficiency of initiation from all six sites of the hexafunctional initiator.

While past attempts to synthesize well-controlled star polymers by ATRP are limited to $\bar{M}_w$ lower than 600 000,[13,24] we desired star PMMA of much higher molecular weight for potential application as solution

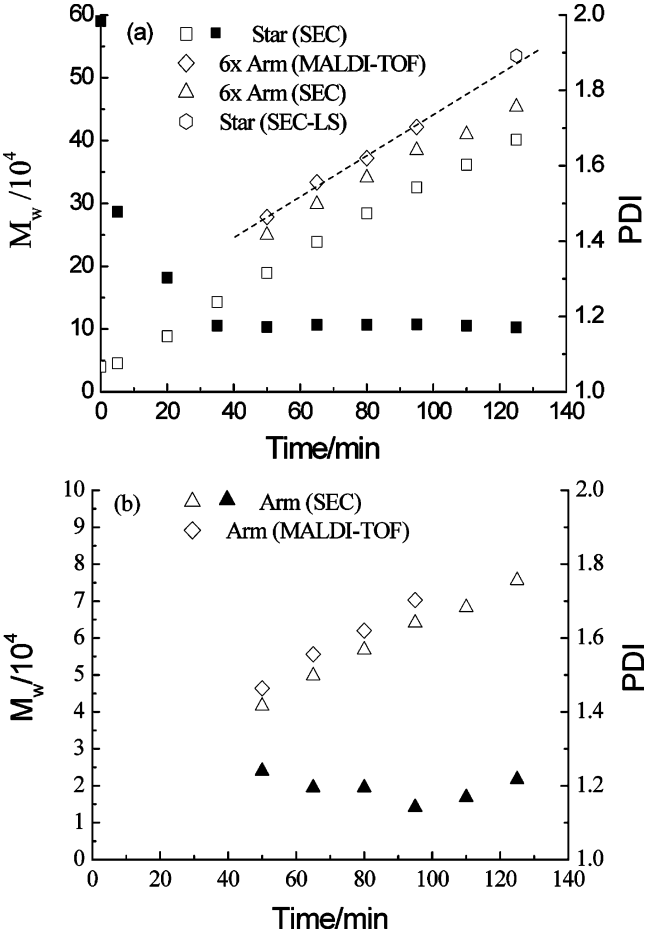

Figure 3. $\bar{M}_w$ (empty symbols) and PDI ($=\bar{M}_w/\bar{M}_n$) (filled symbols) of PMMA formed at different times during the polymerization with monomer-to-initiating site ratio ($[M]_o/[I]_o$ = 3400), (a) fused-core star PMMA by SEC and SEC-LS and the comparison with six times the molecular weight of their cleaved arms, (b) the cleaved arms by SEC and MALDI-TOF-MS. The dashed line in (a) is the linear fit to the MALDI-TOF-MS data.

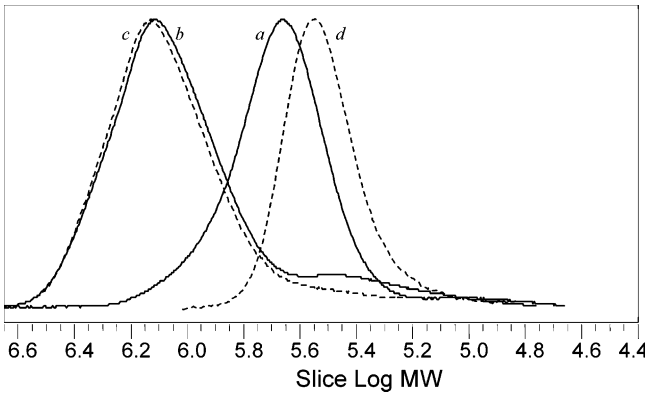

Figure 4. SEC traces of high-molecular-weight fused-core star PMMA formed at different times during the $[M]_o/[I]_o = 16\,333$ polymerization. Solid lines *a* and *b* represent samples withdrawn during the polymerization at 61 and 265 min, respectively. Dashed line *c* represents precipitation fractionation product of *b*. Dashed line *d* represents the cleaved arm of *c*.

rheology modifier. For this, we carried out the ATRP while using a much higher $[M]_o/[I]_o$ (= 16 333). As seen in Figure 4, the SEC peaks of the samples withdrawn during ATRP shifted to higher molecular weights while retaining narrow width. This indicates that the ATRP proceeded in a controlled manner. The final sample at

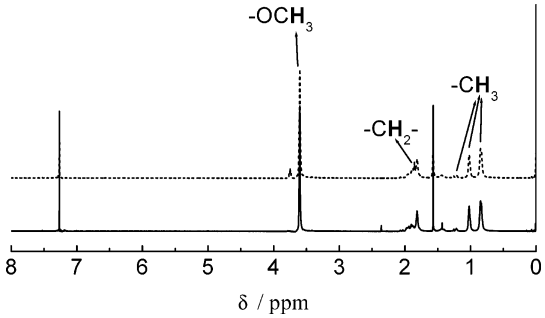

Figure 5. ^{1}H NMR spectra of star PMMA (solid line, corresponding to Figure 4 dashed line *c*) and the cleaved arms (dashed line, corresponding to Figure 4 dashed line *d*).

265 min ($\bar{M}_w \approx 1.32$ million, DPI ≈ 1.30 by SEC) was also analyzed by SEC-LS and found to have $\bar{M}_w \approx 2.35$ million. We do notice a small and broad peak at the low-molecular-weight end. This peak appeared at an early stage during the ATRP, as seen in Figure 4 *a* (t = 61 min). Shifting of this minor peak also to higher molecular weights with progress of reaction (Figure 4 *b*) suggests that this may correspond to a small fraction of linear PMMA chains formed by chain transfer reactions. However, this apparent linear fraction could be easily removed (Figure 4 *c*) by a subsequent purification by precipitation fractionation, as described in the Experimental Section. This final star PMMA sample (Figure 4 *c*) was also subjected to cleavage of the arms, and the arms were analyzed by SEC (Figure 4 *d*, $\bar{M}_w \approx$ 339 700, PDI $\approx$ 1.16). Considering the possible limitation of the universal calibration employed in SEC, the arm molecular weight was further analyzed by SEC-LS. The so-determined $\bar{M}_w$ of 360 000 corresponds reasonably well to the expected value 390 000 for a six-arm star PMMA of $\bar{M}_w \approx 2.35$ million and thus indicates a well-controlled six-arm star architecture of this very high-molecular-weight fused-core star PMMA.

As in our earlier work with linear PMMA,[16] control was achieved here by maximizing the initiation efficiency and minimizing the inter- and intramolecular termination of the growing species by (a) using very high monomer-to-initiating site ratio ($[M]_o/[I]_o$), (b) predilution of the initiator core before adding into the polymerization flask, (c) halogen exchange to speed up initiation, and slow propagation, and (d) limiting our polymerizations to low monomer conversion.

^{1}H NMR (400 MHz) spectra of the original star PMMA and the cleaved arms are shown in Figure 5; the chemical shifts at 0.84, 1.02, and 1.2 ppm correspond to the syndiotactic, heterotactic, and isotactic methyl protons ($-CH_3$), respectively.[25] The signal at 3.60 ppm corresponds to the ester protons ($-OCH_3$). As expected, the area ratio of these two types of protons is 1 for both the star PMMA and the cleaved-arm samples.

ATRP of Linear-Core Star PMMA. High-molecular-weight linear-core star PMMA were synthesized from the hexafunctional initiator EG(Bz3Br)$_2$ as shown in Scheme 2 by ATRP of MMA with high $[M]_0/[I]_0$ (=19 074). Similar to the case of fused-core star PMMA, the SEC peaks of the linear-core star PMMA samples shifted to increasing molecular weights with increasing reaction times (Figure 6a), while retaining narrow width, again indicating the controlled nature of the ATRP reaction. The corresponding $\bar{M}_w$ and PDI values are shown in Figure 6b. The final sample at 240 min ($\bar{M}_w \approx 1.19$ million, PDI ≈ 1.26 by SEC) was analyzed

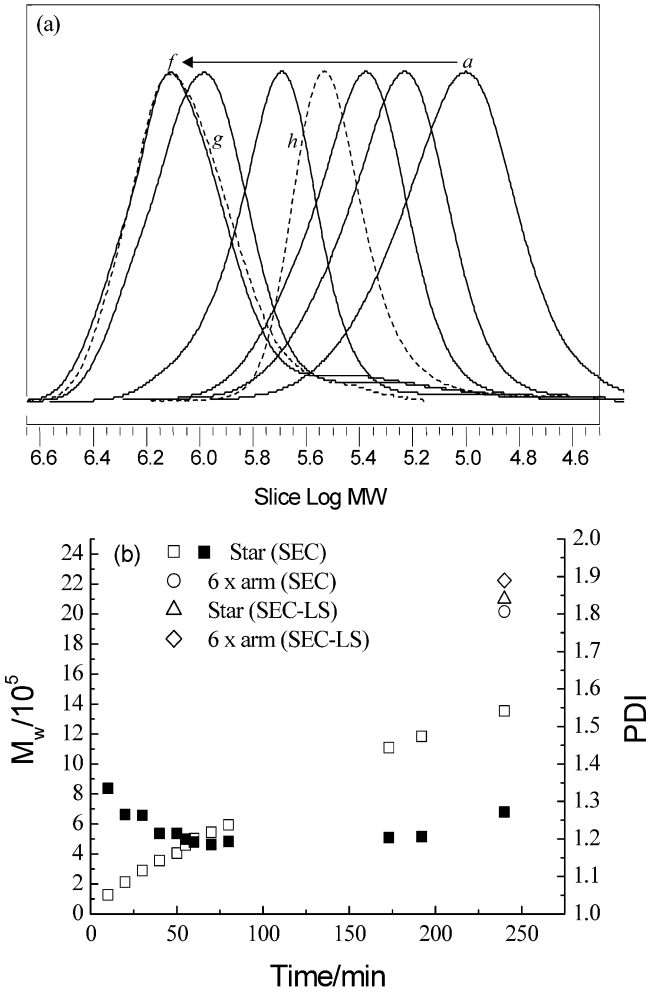

Figure 6. SEC traces (a), weight-average molecular weight (empty symbols) and polydispersity index (filled symbols), and the comparison with six times the molecular weight of their cleaved arms (b) of the linear-core star PMMA formed at different times during the progress of ATRP using high ($[M]_o/[I]_o = 19\,074$). Solid lines represent samples withdrawn during the polymerization at following times: *a*, 10 min; *b*, 20 min; *c*, 30 min; *d*, 80 min; *e*, 173 min; and *f*, 240 min. Dashed line *g* represents the precipitation fractionation product of the 240 min sample (curve *f*). Dashed line *h* represents cleaved arms of the fractionated star PMMA (curve *g*).

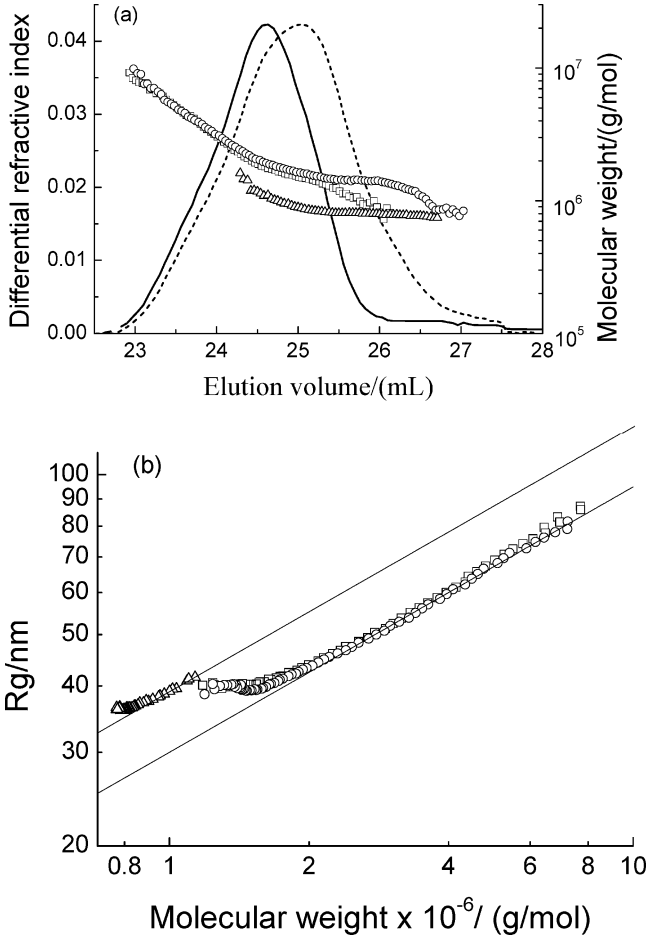

Figure 7. SEC-LS characterization of PMMA samples. Triangles, linear PMMA reference; squares, fused-core star PMMA (curve *c* of Figure 4); circles, linear-core star PMMA sample (curve *g* of Figure 6a). (a) Molecular weight (symbols) and concentration distribution (lines) vs elution volume. The solid line represents fused-core star PMMA, and the dashed line represents linear-core star PMMA. (b) Radius of gyration vs molecular weight. The lowest MW data for the star polymers overlap with those of the linear reference sample and have been removed for clarity. The solid lines represent power law with 0.5 exponent.

by SEC-LS and found to have $\bar{M}_w \approx 2.1$ million. Similar to the fused-core star PMMA case (Figure 4, samples *a* and *b*), the last two samples in Figure 6a also show minor peaks at low molecular weight, shifting to higher molecular weights during the polymerization. Again, this low-molecular-weight peak was easily removed by precipitation fractionation (dashed line *g* of Figure 6a). This linear-core star PMMA sample was then subjected to cleavage into arms, which were analyzed by SEC (dashed line *h* of Figure 6a, $\bar{M}_w \approx 336\,100$, PDI ≈ 1.18) and SEC-LS ($\bar{M}_w \approx 370\,000$). These values compare well with the value 350 000 expected on the basis of six-arm star PMMA of $\bar{M}_w \approx 2.1$ million.

Molecular Characteristics of the Star PMMAs by SEC-LS. Shapes of the polymer molecules in solution are best investigated by combined measurements of radius of gyration (R_g, z-average) and absolute molecular weight (MW, weight average) by light scattering of fractions eluting during SEC.[26] In Figure 7, we compare these characteristics of our very high-molecular-weight fused-core and linear-core star PMMA samples with a linear PMMA reference. Star PMMA samples have higher MW compared to linear PMMA at the same hydrodynamic volume (assumed to correspond to elution volume, V_e) as shown in Figure 7a. The change in slope of the MW/V_e curves for both the linear and the star PMMA at $V_e \approx 24-25$ mL is related to the column characteristics. The concentration signals from both star polymers are also shown in the same figure, and we notice that, over the central part of the star polymer distributions, the MW ratio at identical hydrodynamic volume of linear and star molecules remains essentially constant (~1.7). This value is higher than the 1.48 figure predicted by the Cassasa formula (eq 1). The discrepancy can be due to one or more of the following. First, the linear PMMA used as reference has been anionically polymerized and therefore has different tacticity and, hence, a different hydrodynamic radius vs MW relationship than the PMMA synthesized by ATRP. Second, excluded volume effects (THF is not a theta solvent for PMMA), unaccounted for by eq 1, could also play a role. Third, eq 1 may have additional dependence on pore size and arm length near the exclusion limit of the SEC columns.[23]

At the low end of the molecular weight distributions corresponding to elution volume greater than 25.5 and

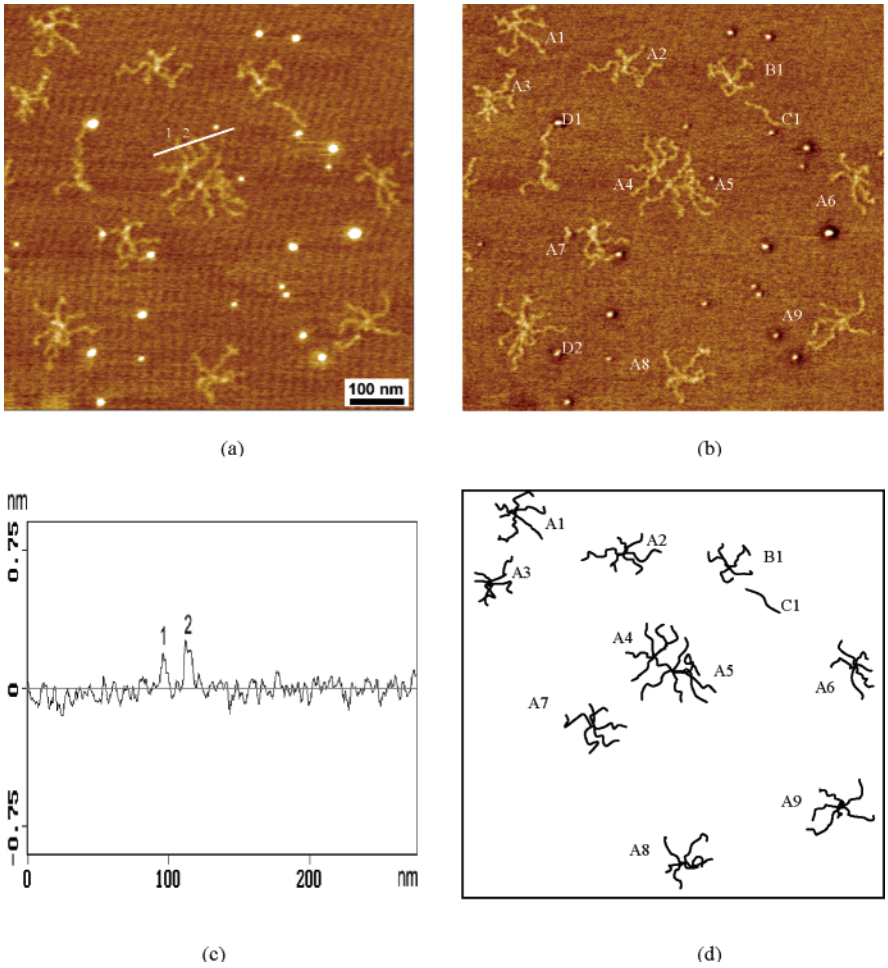

Figure 8. SFM Tapping Mode images of star PMMA ($\bar{M}_w \approx 535\,000$, by SEC-LS) on mica: (a) height image (z-range: 1.8 nm); (b) phase image (z-range: 15°); (c) the height profile of two PMMA arms along the solid line indicated in (a); (d) schematic representation of the possible molecular conformations of labeled star molecules in (a) and (b).

26 mL for the fused-core and linear-core star PMMA, respectively, the MW vs V_e curves of the star polymers deviate toward the linear reference curve (Figure 7a). This could be related to a small extent of incomplete ATRP initiation resulting in fewer arms or a small extent of chain-transfer reactions resulting in some smaller arms and some linear chains, as was also inferred from the SEC observations (Figures 4 and 6a). Figure 7b shows that most of the star PMMA samples have lower R_g than linear PMMA of same MW. The close overlap of the linear core and fused core star PMMA characteristics in Figure 7a and b indicates a similar branching topology for these two samples. Over the main part of the molecular weight distribution of the star polymers, the R_g/MW relationship follows a power law with an exponent very close 0.5 (Figure 7b). The discrepancy below 1.4 million, for the star R_g/MW relationship with an exponent lower than 0.5, may be due to some star molecules of fewer arms or some linear chains, leading to a less compact conformation. If intermolecular coupling of star polymers takes place during polymerization, the coupled product should be discernible as a prominent high-molecular-weight shoulder in the concentration signal.[12,23] However, the SEC peaks (Figures 4, 6a, and 7a) are fairly symmetric and devoid of any distinct shoulder. Moreover, the exponent of the R_g vs MW power law must be affected by coupling, if present. Only the slightest hint of such a crossover can be observed at the highest MW in Figure 7b for the fused-core star PMMA, while the power law extends to the highest MW fraction for the linear-core star PMMA. We can thus conclude that the star-star coupling was virtually eliminated during our ATRP, perhaps due to the termination of polymerization at low conversion (less than 0.2).

SFM Visualization of Branching Topology of Star PMMA. In recent years, SFM has emerged as a very useful tool for direct visualization of isolated linear polymer molecules.[27] The technique has also been employed for visualization of star and branched polymers but only after dense grafting to enhance the backbone feature width[27−30] or metallization to enhance the contrast.[31,32] As shown in Figure 8, we managed to visualize the branch architecture by directly fixing the star-PMMA molecules ($\bar{M}_w \approx 535\,000$ by SEC-LS, the final sample in Figure 3a) on mica substrate in an isolated form by dip-coating from a very dilute solution in THF. We believe that the mobility of the PMMA chains was limited by the interaction of the ester groups of PMMA with the polar mica substrate. In addition, fast evaporation of the solvent helped avoid the aggregation of the arm-branches. The height profile in Figure 8c permits the estimation of the thickness of the arm-branches as about 0.2 nm. The SFM images in Figure 8 allows us to count the numbers of arms in individual star molecules, such as six arms for the molecules labeled A1−A9, five arms for the molecule labeled B1. As shown further in Figure 8d as the schematic sketch of Figure 8a and b, the majority of the star PMMA molecules have six arms. The molecules A4

and A5 appear at first sight to be a case of intermolecular coupling between arms of the two molecules, but that would have resulted in detection of 11 independent arms. However, a close examination reveals 12 arms for the two molecules, indicating a simple overlapping during the coating process as one arm of the molecule A4 happens to reach the core of molecule A5. For some cases such as D1, a judgment of the number of arms is made ambiguous by the apparent overlapping of arms.

Intramolecular coupling, incomplete initiation, and transfer reactions at the early stage of the polymerization may result in the four-arm star, five-arm star, and linear molecules. However, the extent of such reactions is limited. For example, we find only one linear chain (C1) in Figure 8 among a total of 12 star molecules, i.e., about 1.4% based on the initiating sites. Because of the finite dimension of the SFM tip (radius ca. 10 nm), small folds of the flexible chains on the mica substrate could not be resolved, and thus apparent arm contour lengths in Figure 8 are smaller than the expected 228 nm for fully extended arms of molecular weight 91 000.

Conclusions

Six-arm star PMMAs with two different core structures were synthesized by core-first ATRP. While in the linear core star PMMA, two sets of three arms each were linked with a linear segment, all six arms in the fused-core star PMMA were independently connected to a central fused ring structure. Molecular weight characterization of the star PMMA and the cleaved arms indicated that the ATRP initiated from all the six initiating sites of the specially synthesized hexafunctional initiators and proceeded in a controlled manner. Star PMMAs of molecular weight higher than 2 million, and low polydispersity, were thus obtained while using very high $[M]_o/[I]_o$ and terminating the reaction at low monomer conversion. The smaller R_g of the star PMMA as compared to linear PMMA of same molecular weight and a power law relationship between R_g and molecular weight confirmed the compact and regular structure of the star PMMA. Isolated molecules of ATRP product were visualized by tapping mode SFM, and most of these clearly showed the six-arm star PMMA architecture.

Acknowledgment. We thank Wieb Kingma for SEC measurements and Pascal van Velthem for SEC-LS measurements.

References and Notes

(1) *Polymers as Rheology Modifiers*; Schultz, D. N.; Glass, J. E. Eds.; ACS Symposium Series 462; American Chemical Society: Washington, DC, 1991.
(2) Gao, C.; Yan, D. *Prog. Polym. Sci*. **2004**, *29*, 183.
(3) McLeish, T. C. B. *Trans. IchemE* **2000**, *78*, 12−32.
(4) Agarwal, U. S.; Mashelkar, R. A. *J. Chem. Phys.* **1994**, *100*, 6055.
(5) Kulicke, W. M.; Kotter, M., Grager, H. *Adv. Polym. Sci.* **1989**, *89*, 1.
(6) Madkour, T. M.; Mark, J. E. *Polym. Bull.* **1997**, *39*, 385.
(7) Loveday, D.; Wilkes, G. L.; Lee, Y.; Storey, R. F. *J. Appl. Polym. Sci.* **1997**, *63*, 507.
(8) Storey, R. F.; Chisholm, B. J.; Masse, M. A. *Polymer* **1996**, *37*, 2925.
(9) Matyjaszewski, K.; Miller, P. J.; Fossum, E.; Nakagawa, Y. *Appl. Oganomet. Chem.* **1998**, *12*, 667.
(10) Kasko, A. M.; Heintz, A. M.; Pugh, C. *Macromolecules* **1998**, *31*, 256.
(11) Ueda, J.; Kamigaito, M.; Sawamoto, M. *Macromolecules* **1998**, *31*, 6762.
(12) Angot, S.; Murthy, K. S.; Taton, D.; Gnanou, Y. *Macromolecules* **1998**, *31*, 7218.
(13) Matyjaszewski, K.; Miller, P. J.; Pyun, J.; Kickelbick, G.; Diamanti, S. *Macromolecules* **1999**, *32*, 6526.
(14) Huang, C.; Lee, H.; Kuo, S.; Xu, H.; Chang, F. *Polymer* **2004**, *45*, 2261.
(15) Heise, A.; Diamanti, S.; Hedrick, J. L.; Frank, C. W.; Miller, R. D. *Macromolecules* **2001**, *34*, 3798−3801.
(16) Xue, L.; Agarwal, U. S.; Lemstra, P. J. *Macromolecules* **2002**, *35*, 8650.
(17) Beuermann, S.; Paquet, D. A., Jr.; McMinn, J. H.; Hutchinson, R. A. *Macromolecules* **1996**, *29*, 4206. Kirkland, J. J.; Rementer, S. W. *Anal. Chem.* **1992**, *64*, 904.
(18) (18) *Polymer Handbook*, 3rd ed.; Brandrup, J., Immergut, E. H., Eds.; Wiley-Interscience: London, 1989; Section VII, p 432.
(19) Beattie, D. R.; Hindmarsh, P.; Goodby, J. W.; Haslam, S. D.; Richardson, R. M. *J. Mater. Chem.* **1992**, *2*, 1261−1266.
(20) Mori, S.; Barth, H. G. *Size Exclusion Chromatography*; Springer Verlag: Berlin Heidelberg, New York, 1999.
(21) Rudin, A.; Grinshpun, V.; O'Driscoll, K. *J. Liq. Chromatogr.* **1984**, *7*, 1809.
(22) Radke, W. *Macromol. Theory Simul.* **2001**, *10*, 668.
(23) Radke, W.; Gerber, J.; Wittmann, G. *Polymer* **2003**, *44*, 519.
(24) Feng, X.; Pan, C. *J. Polym. Sci., Part A: Polym. Chem.* **2001**, *39*, 2233−2243.
(25) Fuchs, K.; Friedrich, Chr.; Weese J. *Macromolecules* **1996**, *29*, 5893.
(26) Sun, T.; Chance, R. R.; Graessley, W. W.; Lohse, D. J. *Macromolecules* **2004**, *37*, 4304.
(27) Sheiko, S. S.; Möller, M. *Chem. Rev.* **2001**, *101*, 4099−4123.
(28) Kumaki, J.; Nishikawa, Y.; Hashimoto, T. *J. Am. Chem. Soc.* **1996**, *118*, 3321−3322.
(29) Sheiko, S. S.; Prokhorova, S. A.; Beers, K. L.; Matyjaszewski, K.; Potemkin, I. I.; Khokhlov, A. R.; Möller, M. *Macromolecules* **2001**, *34*, 8354−8360.
(30) Cheng, G.; Böker, A.; Zhang, M.; Krausch, G.; Müller, A. H. E. *Macromolecules* **2001**, *34*, 6883−6888.
(31) Gorodyska, G.; Kiriy, A.; Minko, S.; Tsitsilianis, C.; Stamm, M. *Nano Lett.* **2003**, *3*, 365−368.
(32) Kiriy, A.; Gorodyska, G.; Minko, S.; Stamm, M.; Tsitsilianis, C. *Macromolecules* **2003**, *36*, 8704−8711.

MA0484936